

CHARACTERISTICS OF SURFACE ACOUSTIC WAVES PROPAGATING OBLIQUELY IN PERIODIC ELECTRODE GRATINGS

Vincent Laude and Sylvain Ballandras

Laboratoire de Physique et de Métrologie des Oscillateurs, CNRS UPR 3203, associé à l'Université de Franche-Comté, Besançon, France

The characteristics of surface acoustic waves (SAW) propagating obliquely in electrode gratings are investigated, with the mass-loading effect taken into account. The velocity of the surface waves, as well as the attenuation, piezoelectric coupling and beam-steering are obtained as a function of the propagation angle with respect to the grating axis. The slowness curves for SAW propagating under periodic electrode gratings are compared with slowness curves for the same SAW propagating on free or shorted homogeneous surfaces as well as under a thick homogeneous metallic layer. Examples are presented for the SAW of 42.75°YX quartz and the leaky-SAW of 36°YX lithium tantalate

Introduction

During the last decade, much work has been devoted to the modeling and the numerical simulation of surface acoustic waves (SAW) propagating under interdigital transducers (IDT), including the mass-loading effect that is due to acoustic propagation inside the aluminum electrodes. These tools are especially useful to understand the wave propagation characteristics in actual SAW filters, and hence are used routinely to obtain the basic parameters required for filter design. They are generally based on a mixed finite element analysis (FEA) / boundary integral method (BIM) [1-4], in which the wave solution in the electrodes and in the substrate are respectively obtained by FEA and a Green's function, and the two domains are related using a BIM to obtain the harmonic admittance.

One limitation of the FEA/BIM method is that for computation reasons the problem is restricted to two dimensions, with the electrodes assumed infinite in the transverse direction. However, real SAW devices are of finite width, and transverse effects occur that can not be taken into account using a 2D model. Though an exact 3D model is probably still beyond reach, useful information can be gained by examining the propagation of slanted acoustic waves in periodic gratings. Indeed, diffraction effects caused by the finite transverse dimension of the electrodes can in principle be addressed by developing the transverse wave structure as a sum over slanted acoustic waves.

In this paper, we address the problem of obtaining the slowness curves for surface acoustic waves propagating in periodic electrode gratings [5], i.e. defining the phase angle θ as the angle of propagation with respect to the electrodes axis, we show how the phase velocity can be obtained as a function of θ , including the mass-loading effect. Along with the phase velocity, we also discuss how other useful information regarding the propagating waves can be obtained as a function of angle θ , e.g. the attenuation, the electro-mechanical coupling and the beam-steering angle.

In order to achieve this goal, we have extended some

standard concepts and methods of SAW propagation analysis so that they apply to slanted waves, including Green's functions analysis, the P-matrix model and the FEA/BIM method. In particular, we will discuss a finite element model suited to our purposes.

Numerical simulation results are presented for some standard piezoelectric substrates widely used for the fabrication of SAW devices, such as ST quartz (true SAW) and Y+36 lithium tantalate (pseudo or leaky SAW). The slowness curves for SAW propagating under periodic electrode gratings are compared with slowness curves for the same SAW propagating under a thick homogeneous metallic layer.

Slowness Curves

We first discuss here how the slowness curves can be exploited to obtain the beam-steering and the diffraction parameter in a periodic electrode grating. In the case of a free or shorted surface, and also in the case of a uniform metallic layer deposited on the piezoelectric substrate, the beam-steering is best obtained via the Poynting vector, which is known to be normal to the slowness curve and can be obtained rather simply. In the case of a periodic electrode grating however, though a Poynting vector can still be defined, it will depend on an infinite number of harmonics of the grating period. Alternatively, the beam-steering can be obtained by numerical differentiation of the slowness curve. Let us assume that we can compute the slowness as a function of the phase angle, i.e. the function $s(\theta)$ in polar coordinates is known, with the angle θ expressed in radians. The coordinates of a running point on the slowness curve is then

$$\begin{pmatrix} x(\theta) \\ y(\theta) \end{pmatrix} = \begin{pmatrix} s(\theta)\cos(\theta) \\ s(\theta)\sin(\theta) \end{pmatrix} \quad (1)$$

from which the tangent at that point is

$$\begin{pmatrix} x'(\theta) \\ y'(\theta) \end{pmatrix} = \begin{pmatrix} s'(\theta)\cos(\theta) - s(\theta)\sin(\theta) \\ s'(\theta)\sin(\theta) + s(\theta)\cos(\theta) \end{pmatrix} \quad (2)$$

The beam steering angle ψ is defined as the angle between the normal to the slowness curve and the phase direction. Expressing this condition and after some simple algebra, we arrive at

$$\begin{pmatrix} \cos \psi \\ \sin \psi \end{pmatrix} = \frac{1}{d(\vartheta)} \begin{pmatrix} 1 \\ -g(\vartheta) \end{pmatrix} \quad (3)$$

with the definitions

$$g(\vartheta) = \frac{d}{d\vartheta} \log s(\vartheta) = \frac{s'(\vartheta)}{s(\vartheta)} \quad (4)$$

and

$$d(\vartheta) = \sqrt{1 + g^2(\vartheta)} \quad (5)$$

From Eqs. (3-5), the beam-steering angle can be computed by evaluating the first derivative of the slowness curve.

By definition, the diffraction parameter is

$$\gamma(\vartheta) = \frac{d\psi(\vartheta)}{d\vartheta} \quad (6)$$

Since the beam-steering angle is obtained as a first derivative, the diffraction parameter is obtained as a second derivative of the slowness curve, and can be expressed as

$$\gamma(\vartheta) = \frac{-g'(\vartheta)}{1 + g^2(\vartheta)} \quad (7)$$

SAW Parameters Estimation

In the process of computing slowness curves for surface waves, it is necessary to locate the slowness as a function of the propagation angle θ in the surface plane. Fig. 1 illustrates the notations employed. The actual algorithm employed will depend on the nature of the propagation problem. On a free or shorted surface, the wave characteristics are functions of the material constants only, and are not dispersive. Under a metallic grating however, the wave characteristics are dispersive, i.e. they depend on the frequency period product fp , but in addition they also depend on the electrodes shape, which for a rectangular electrode is scaled by the form factor $h/2p$, where h is the electrode height. For propagation under a thick metallic layer deposited upon the piezoelectric substrate, the wave characteristics are also dispersive, and depend on the frequency thickness product fh , where h is now to be understood as the layer thickness.

In the case of an homogeneous surface with either free or shorted boundary conditions, it is well-known that the slowness is given respectively by a pole or a zero of the so-called effective permittivity. Such an approach has been used routinely to obtain maps of surface waves parameters [6]. The effective permittivity is a restriction of the Green's function of the semi-infinite substrate to its electrical components [7]. The computation of the surface Green's function in the spectral domain has for instance been described in Ref. [8].

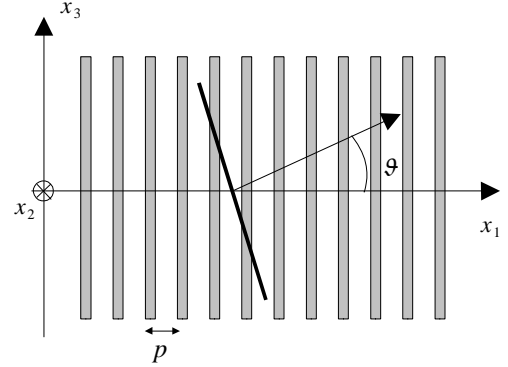


Fig. 1: Geometry for slanted SAW propagation in a periodic metallic grating.

In the case of periodic electrode gratings, two additional phenomena have to be accounted for, namely the frequency dependence arising from the periodic perturbation of the surface and the periodic electrical excitation of waves, and the so-called mass-loading effect of the electrodes. The first phenomenon is adequately described (at least as regards the electrical part of the problem) using the notion of the strip admittance [9], extended to the notion of harmonic admittance (HA) in Ref. [7]. The occurrence of a piezoelectrically coupled surface wave is then given by a pole of the HA. There have been many approaches to the computation of the mass-loading effect, with most of them relying on a finite element analysis (FEA) of the acoustical propagation in the electrodes [1-4]. In this work, we have used the approach described in [3], which is a combination of a FEA for the electrodes with a BIM relying upon the Green's function of the semi-infinite substrate. We describe in Appendix A how the classical finite element approach can be modified to accommodate for slanted propagation.

It has been shown [7] that the contribution of a SAW to the HA takes the following approximate form

$$Y_s(\gamma) = \frac{jY_0}{\tan(\phi_s)/2} \frac{1 - \cos(2\pi\gamma)}{\cos(\phi_s) - \cos(2\pi\gamma)} \quad (8)$$

where γ is the driving parameter of the harmonic excitation potential

$$V(\gamma) = \exp(2j\pi\gamma) \quad (9)$$

In Eq. (8), ϕ_{sc} is the phase delay per grating period, from which the slowness is obtained as

$$s = \frac{\phi_s}{2\pi f p} \quad (10)$$

from which the attenuation is obtained if the phase delay is considered complex. The static capacitance contribution to the HA is of the form

$$Y_c(\gamma) = C \sin(\pi\gamma) \quad (11)$$

and the total HA is modelled as

$$Y(\gamma) = Y_s(\gamma) + Y_c(\gamma) \quad (12)$$

Thereby the contribution of bulk waves is neglected. The

unknown parameters ϕ_{sc} , Y_0 and C are estimated via a fit of the model (12) to the numerical simulation of the HA obtained using the FEA/BIM method. Most quantities plotted in the next section are rather well defined, i.e. the velocity at resonance (the inverse of the slowness), the attenuation, the beam-steering angle and the diffraction parameter, but this is not true for the coupling strength. It is customary to employ the $K^2 = 2 \Delta v / v$ for this purpose, however this is defined solely for propagation on either a free or a shorted surface, and is moreover adequate only for a lossless SAW, i.e. does not apply to a leaky SAW. The coupling strength used to plot Figs. (5) and (10) is the ratio Y_0/C , and should be considered only to have a relative significance.

Simulation Examples

All results presented in this section are obtained for an infinite periodic electrode grating on a semi-infinite piezoelectric substrate. The zero phase angle refers to propagation along the grating axis. All parameters given are those obtained for a pole or pseudo-pole of the harmonic admittance, i.e. for the resonance condition, with the frequency period product fp set to 1000 m/s, i.e. far from the stop-band in all cases.

The denomination for the considered ST cut of quartz is (YXl)/42.75 in the IEEE 1949 piezoelectric standard. The dependence of the slowness, beam-steering, diffraction parameter and piezoelectric coupling for the SAW of ST quartz are depicted in Figs. 2, 3, 4 and 5 respectively, for three values of the electrode aspect ratio $h/2p$ (0, 5 and 10 %). The slowness is seen to be rather strongly affected by the mass loading effect, as is well-known for ST quartz, and to assume a symmetrical and mostly parabolic shape. The beam-steering remains limited, while the coupling increases with the phase angle. It should be noted that no attenuation was found to occur at any angle.

The denomination for the considered cut of lithium tantalate is (YXl)/36 in the IEEE 1949 piezoelectric standard. This cut is famous for its leaky SAW, or pseudo SAW (PSAW). The dependence of the slowness, attenuation, beam-steering and piezoelectric coupling for the PSAW are depicted in Figs. 6, 7, 8 and 9 respectively, for three values of the electrode aspect ratio $h/2p$ (0, 5 and 10 %). The slowness is seen to be much less affected by the mass loading effect than is that of the SAW of ST quartz, and to assume a parabolic shape. The beam-steering varies rather largely with the phase angle. The coupling is maximum along the grating axis, while at the same time the attenuation is at a minimum.

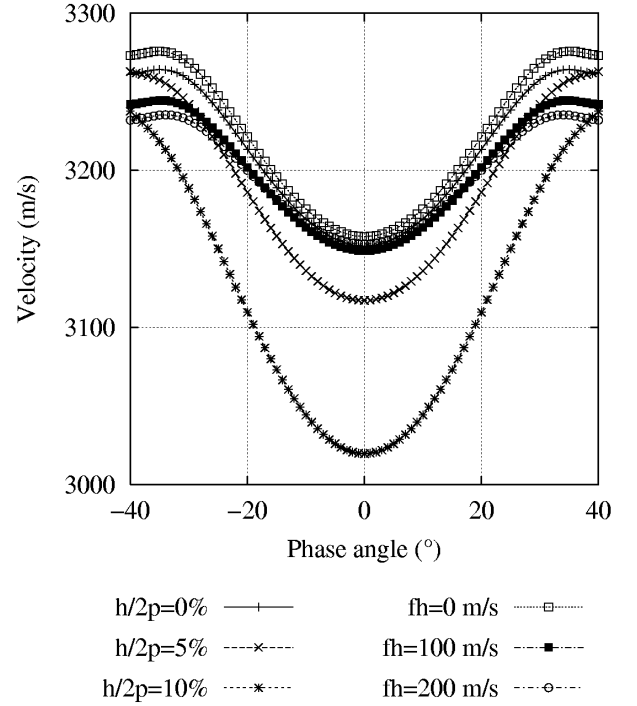


Fig. 2: Velocity of the SAW of ST quartz under an aluminum layer and in a periodic grating ($fp=1000$ m/s).

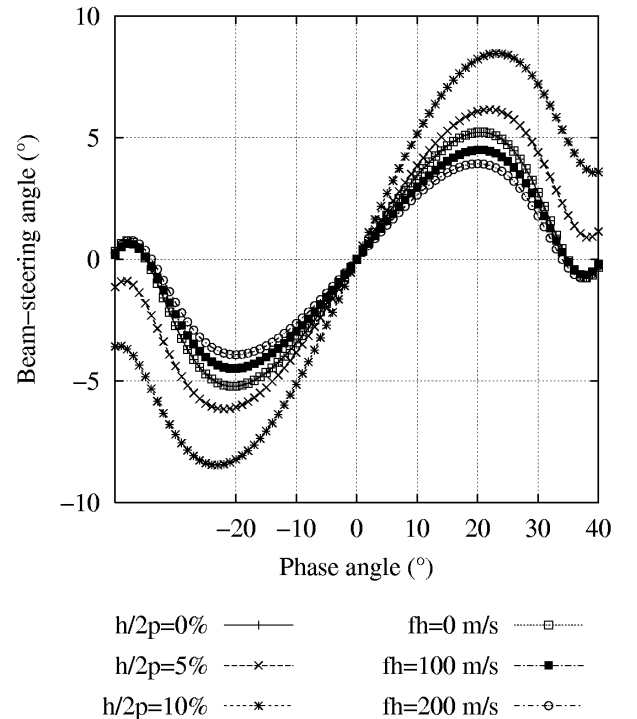


Fig. 3: Beam-steering of the SAW of ST quartz under an aluminum layer and in a periodic grating ($fp=1000$ m/s).

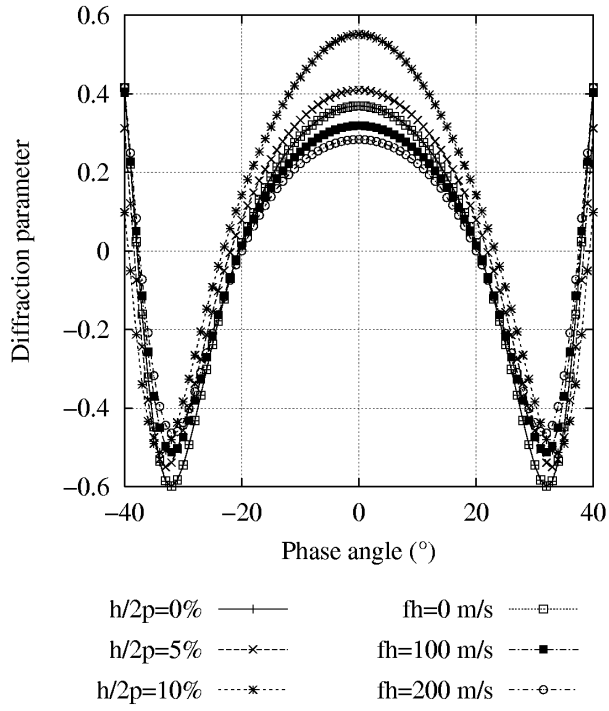


Fig. 4: Diffraction parameter γ of the SAW of ST quartz under an aluminum layer and in a periodic grating ($fp=1000$ m/s).

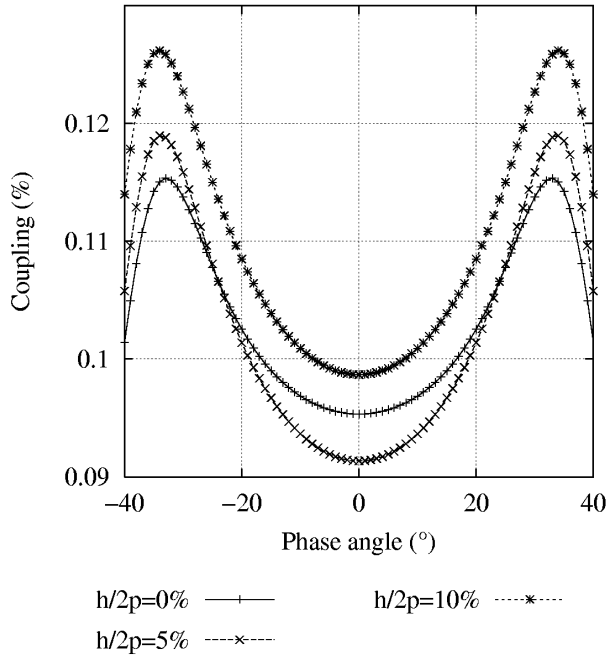


Fig. 5: Coupling strength of the SAW of ST quartz in a periodic grating ($fp=1000$ m/s); see text for comments about the definition of the coupling strength.

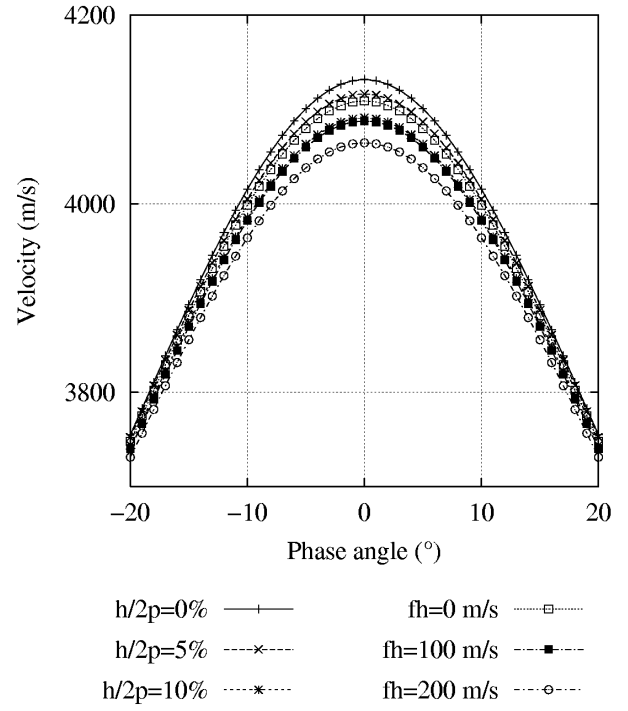


Fig. 6: Velocity of the leaky-SAW of 36° YX lithium tantalate under an aluminum layer and in a periodic grating ($fp=1000$ m/s).

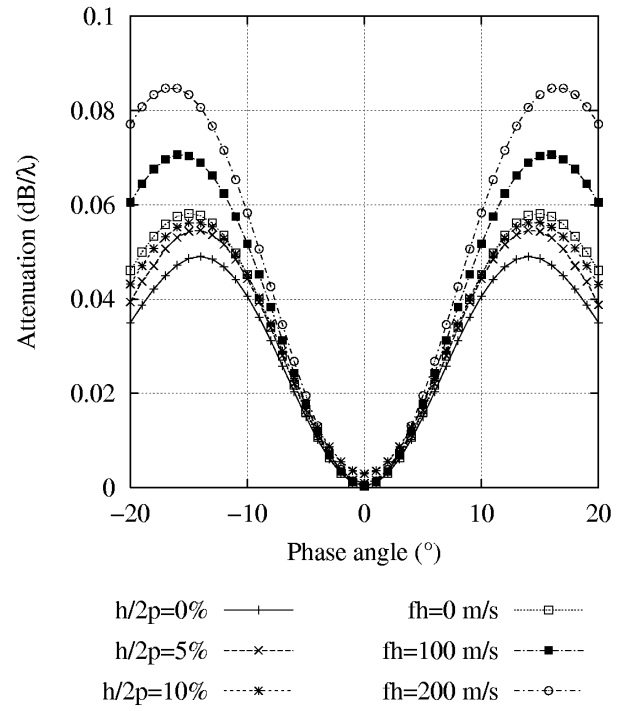


Fig. 7: Attenuation of the leaky-SAW of 36° YX lithium tantalate under an aluminum layer and in a periodic grating ($fp=1000$ m/s).

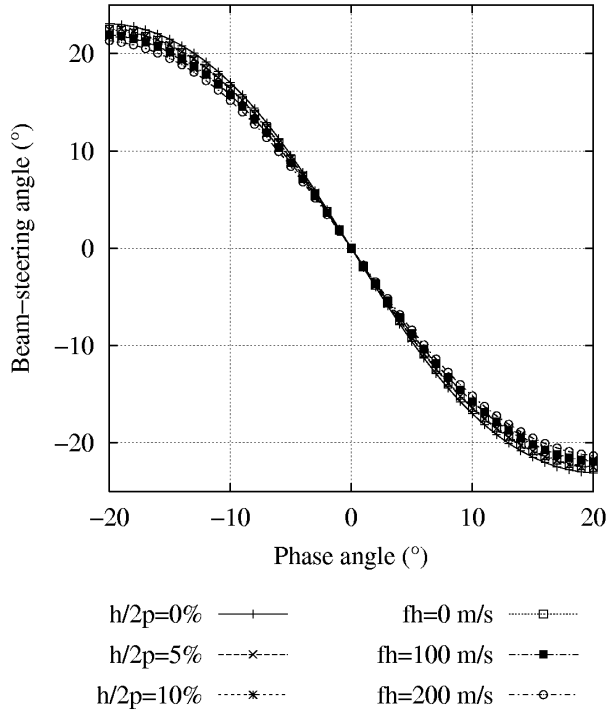


Fig. 8: Beam-steering of the leaky-SAW of 36°YX lithium tantalate under an aluminum layer and in a periodic grating ($f_p=1000$ m/s).

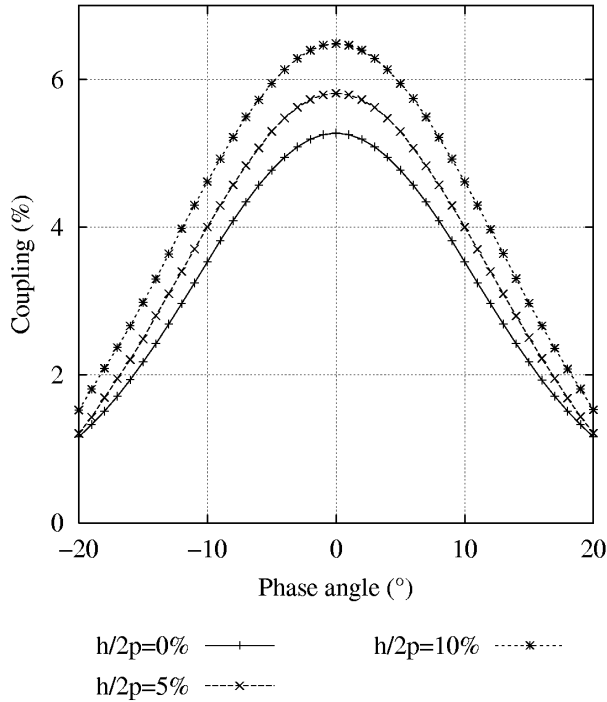


Fig. 9: Coupling strength of the leaky-SAW of 36°YX lithium tantalate in a periodic grating ($f_p=1000$ m/s); see text for comments about the definition of the coupling strength.

Conclusion

The characteristics of surface acoustic waves propagating obliquely in electrode gratings have been investigated, with the mass-loading effect taken into account. The slowness of the surface waves, as well as the attenuation, piezoelectric coupling and beam-steering have been obtained as a function of the propagation angle with respect to the grating axis. The method is based on the monitoring of poles in the harmonic admittance, which is computed using a FEA/BIM approach. A modification of classical finite element analysis was derived to account for slanted propagation. Examples were presented for 42.75°YX quartz and 36°YX lithium tantalate.

The authors acknowledge fruitful discussions with J. Desbois, M. Solal and P. Ventura of Thales Microsonics, France.

References

- [1] M. Buchner, W. Ruile, A. Dietz and R. Dill, "FEM analysis of the reflection coefficient of SAWs in an infinite periodic array," IEEE Ultrason. Symp. Proc., 371-375 (1991).
- [2] H. P. Reichinger and A. R. Baghai-Wadji, "Dynamic 2D analysis of SAW devices including mass-loading," IEEE Ultrason. Symp. Proc., 7-10 (1992).
- [3] P. Ventura, J.-M. Hodé and J. Desbois, "A new efficient combined FEM and periodic Green's function formalism for the analysis of periodic SAW structures," IEEE Ultrason. Symp. Proc., 263-266 (1995).
- [4] G. Endoh, K. Hashimoto and M. Yamaguchi, "Surface acoustic wave propagation characterization by finite element method and spectral domain analysis," Jpn. J. Appl. Phys. **34**, 2638-2641 (1995).
- [5] K. Hashimoto, G. Endoh, M. Ohmaru and M. Yamaguchi, "Analysis of SAWs obliquely propagating under metallic gratings with finite thickness," Jpn. J. Appl. Phys. **35**, 3006-3009 (1996).
- [6] A. L. Slobodnik, E. D. Conway and R. T. Delmonico, Eds., Microwave acoustic handbook, Volume 1A (1973).
- [7] Y. Zhang, J. Desbois and L. Boyer, "Characteristic parameters of surface acoustic waves in a periodic metal grating on a piezoelectric substrate," IEEE Trans. on Ultrason. Ferroelec. Freq. Control **UFFC-40**, 183-192 (1993).
- [8] R. C. Peach, "A general Green function analysis for SAW devices," IEEE Ultrason. Symp. Proc., 221-225 (1995).
- [9] K. Blotekjaer, K. A. Ingebrigtsen and H. Skeie, "A method for analysing waves in structures consisting of metal strips on dispersive media," IEEE Trans. Ultrason. Devices **ED-20**, 1133-1138 (1973).

Appendix A: Finite Element

The finite element that we use was derived from a classical two-dimensional triangle with 3 degrees of freedom, originally intended for isotropic acoustic problems. More precisely, for an infinitely long electrode, the displacements and constraints are usually assumed not to depend on the transverse coordinate x_3 (hence the two-dimensional element), but the 3 components of the

displacement must be taken into account (hence the 3 degrees of freedom). Another possible representation of the finite element is an infinitely long volume with a triangular section. To take into account slanted propagation inside the electrodes, we assume in addition a sinusoidal dependence of the displacements in the transverse coordinate with a given wave-vector k_3 according to

$$\mathbf{u} = \sin(k_3 x_3 + \varphi) [P(x_1, x_2)] \{\mathbf{u}\}_T \quad (\text{A1})$$

where φ is an arbitrary phase. T stands for the finite element considered, P is the polynomial interpolation inside the element, and $\{\mathbf{u}\}_T$ is the vector of coordinates of the nodes. Following the usual procedure of FEA, a variational problem is constructed, which can be cast in a linear form

$$([K] - \omega^2 [M]) \{\mathbf{u}\} = \{\mathbf{B}\} \quad (\text{A2})$$

where $[K]$ is the stiffness matrix, $[M]$ is the mass matrix, ω is the angular frequency and $\{\mathbf{B}\}$ represents the excitation forces applied to the electrode. Using the notations $[P]$ for the polynomial interpolation matrix, $[DP]$ for the matrix of the polynomial derivatives, $[C]$ for the stiffness tensor in contracted notation, ρ for the mass density, and the constant matrices

$$[D] = \begin{pmatrix} 1 & 0 & 0 & 0 & 0 & 0 \\ 0 & 0 & 0 & 1 & 0 & 0 \\ 0 & 0 & 0 & 0 & 0 & 0 \\ 0 & 1 & 1 & 0 & 0 & 0 \\ 0 & 0 & 0 & 0 & 0 & 1 \\ 0 & 0 & 0 & 0 & 1 & 0 \end{pmatrix} \quad (\text{A3})$$

and

$$[D_3] = \begin{pmatrix} 0 & 0 & 0 \\ 0 & 0 & 0 \\ 0 & 0 & 1 \\ 0 & 0 & 0 \\ 0 & 1 & 0 \\ 1 & 0 & 0 \end{pmatrix} \quad (\text{A4})$$

the elementary stiffness and mass matrices can be written respectively as

$$[M_T] = \int_T [P] \rho [P] d\mathbf{x} \quad (\text{A5})$$

and

$$[K_T] = \int_T ([D] [DP]) [C] ([D] [DP]) d\mathbf{x} + \int_T k_3^2 ([D_3] [P]) [C] ([D_3] [P]) d\mathbf{x} \quad (\text{A6})$$

In the derivation, the sinusoidal dependence has dropped by integration along the x_3 axis. By comparison with the usual case of normal propagation ($k_3=0$) it is seen that only the stiffness matrix is affected, and that a positive matrix has to be added to it, weighted by the square of the transverse wave-vector.